Adsorption of Hg(II) from an Aqueous Solution by Silica-Gel Supported Diethylenetriamine Prepared via Different Routes: Kinetics, Thermodynamics, and Isotherms

Rongjun Qu,* Ying Zhang, Changmei Sun, Chunhua Wang, Chunnuan Ji, Hou Chen, and Ping Yin

School of Chemistry & Materials Science, Ludong University, Shandong 264025, China

The kinetics, thermodynamics, and isotherms of Hg(II) ion adsorption onto silica-gel supported diethylenetriamine adsorbents, SG-HE-dD, SG-HO-dD, SG-HE-pD, and SG-HO-pD (where SG means silica-gel; HE, heterogeneous; HO, homogeneous; d, direct; p, protection; and D, diethylenetriamine), prepared by so-called heterogeneous-direct amination, homogeneous-direct amination, heterogeneous end-group protection, and homogeneous end-group protection methods, respectively, were investigated. The results showed that the adsorption processes of Hg(II) ions followed well a pseudofirst-order model onto SG-HE-dD, SG-HO-dD, and SG-HE-pD, while a pseudosecond-order model was followed onto SG-HO-pD. Film diffusion might be dominated in the adsorption process of Hg(II) ions onto the four adsorbents. Thermodynamic analysis revealed that the adsorption behaviors of Hg(II) ions onto the four adsorbents were endothermic processes, resulting in higher adsorption capacities at higher temperature. The Langmuir, Freundlich, and Redlich−Peterson models were employed to fit the isothermal adsorption. The results revealed that the linear Langmuir, nonlinear Langmuir, and nonlinear Redlich−Peterson isotherm models are the best-fit models to predict the experimental data. Mercury ions adsorbed on four adsorbents were desorbed effectively at about 5 % thiourea/0.1 mol·L^{-1} HNO_3, and the adsorption capacity of the SG-HO-dD and SG-HO-pD adsorbents can still be maintained at the (98 and 95) % level at the fifth cycles, respectively.

1. Introduction

The discharge of toxic metals from industrial processes has led to Hg(II) ions entering the environment. Treatment of the resulting Hg(II)-laden water drainage is a critical environmental issue due to the potential for Hg(II) ions and other heavy metals to enter drinking water resources. Furthermore, even low levels of mercury can be concentrated to dangerous levels through the natural process of bioaccumulation.

Various techniques, such as adsorption, solvent extraction, and polymeric membranes, are currently being used to remove Hg(II) ions from the environment.[1–4] One of the promising methods is the use of chelating adsorption. Chelating adsorbents are generally efficient in the removal and recovery of Hg(II) ions because of their physical and chemical stabilities.[5] A polymeric matrix is one of the most well-known matrices of chelating adsorbents, but the high cost of the process has limited its use. Low-cost silica-gel is a type of inorganic polymer, serving as a potentially useful candidate for application to fields of matrices of adsorbents due to their particular structure and unique characters of no swelling, good mechanical stability, and rapid kinetics.[6] In addition, their unique large surface area, well-defined pore size and pore shape, and well-modified surface properties have generated considerable interest to fabricate many novel silica-gel-based adsorbents.[7–10]

Among the silica-gel-based chelating adsorbents, the nitrogen-type chelating resins using nitrogen atoms as ligating atoms have excellent adsorption properties for heavy-metal ions.[11–13] Especially the chelating adsorbents containing multiamino-typed functional groups are capable of coordinating to heavy metal ions to form multidentate chelates owing to a great deal of amino groups existing in the molecules, together with their fine hydrophilicity. Linear polyamines of the form $NH_2(CH_2CH_2NH)_{n-1}H$, i.e., ethylenediamine (EDA, $n = 2$), diethylenetriamine (DETA, $n = 3$), triethylenetetramine (TETA, $n = 4$), tetraethylenepentamine (TEPA, $n = 5$), and pentaethylenehexamine (PEHA, $n = 6$), are kinds of water-soluble molecules, and the two or more nitrogen atoms of amino groups on the line-type molecule can produce very strong chelating action. The character of polyamines has attracted the wide attention of investigators, and their application in adsorption separation fields of heavy-metal ions is developing.[14–17] However, a vital problem of intra- and interstrand cross-linking reactions at different amino and imino groups has been ignored, and the steric restrictions on metal chelate formation were brought about. So far, several attempts have been carried out to immobilize multidentate ligands as discrete units to improve the adsorption properties of the adsorbents.[18–20]

Recently, we have prepared silica-gel-supported diethylenetriamine adsorbents via so-called heterogeneous-direct amination, homogeneous-direct amination, heterogeneous end-group protection, and homogeneous end-group protection methods. The obtained products were named SG-HE-dD, SG-HO-dD, SG-HE-pD, and SG-HO-pD, respectively (where SG means silica-gel, HE means heterogeneous, HO means homogeneous, d means direct, p means protection, and D means diethylenetriamine).[21,22] Moreover, we investigated the adsorption of these adsorbents for Hg(II) in aqueous solution and found that the homogeneous method and end-group protection method were beneficial for discrete units. The objectives of the present study were to further evaluate and compare the four types of silica-gel-supported diethylenetriamine adsorbents with different physicochemical

* Corresponding author. Tel.: +86 535 6673982. E-mail: rongjunqu@sohu.com; qurongjun@eyou.com.

10.1021/je900654e
Published on Web 12/08/2009

characteristics for Hg(II) ion adsorption and to understand the corresponding kinetics, isotherms, thermodynamics, and adsorption mechanisms. Understanding the relationship between the structure and adsorption efficiency should help in identifying which form of silica-gel-supported diethylenetriamine is the most promising for Hg(II) ion removal from wastewaters.

2. Experimental Section

2.1. Materials and Methods. Adsorbents SG-HE-dD, SG-HO-dD, SG-HE-pD, and SG-HO-pD with (0.45, 3.64, 0.33, and 1.36) mmol·g^{-1} of N, respectively, were prepared according to the method described in our previous work.[21] All solutions were prepared from analytical grade chemicals and distilled water. An amount of 0.1 mol·L^{-1} of Hg(II) stock solution was prepared by dissolving 3.4264 g of $Hg(NO_3)_2 \cdot H_2O$ in 100 mL of 0.6 % HNO_3. The working solutions with different concentrations of Hg(II) ions were prepared by appropriate dilutions of the stock solution immediately prior to their use. The initial pH of the solution was adjusted to 4.0 according to our previous work.[22] The concentration before and after adsorption of Hg(II) ions was determined using a 932B-model atomic adsorption spectrophotometer (AAS, GBC, Australia), equipped with an air−acetylene flame.

2.2. Adsorption Kinetics. Adsorption kinetics were performed by mixing a 30 mg of silica-gel adsorbents with 20 mL of Hg(II) solution ($5 \cdot 10^{-3}$ mol·L^{-1}, pH 4.0) in a 100 mL Erlenmeyer flask at different temperatures. An amount of 1 mL of the solution was taken at different time intervals, where the residual concentration of Hg(II) ions was determined via AAS.

2.3. Adsorption Isotherms. Complete adsorption equilibrium was obtained by soaking 30 mg of dry adsorbent in a series of flasks containing 20 mL of initial concentrations of Hg(II) ions ranging from (0.625 to 15) mmol·L^{-1} for 240 min. The initial pH of Hg(II) ion solutions was adjusted to 4.0 while keeping the temperature at (20, 30, or 40) °C. The amount of Hg(II) ions adsorbed at equilibrium q, which represents the Hg(II) ions uptake, was calculated according to the following equation

$$q = \frac{(C_0 - C)V}{W} \quad (1)$$

where q is the adsorption amount (mmol·g^{-1}); C_0 and C are the initial and the final concentrations of Hg(II) ions in the aqueous solution, respectively (mmol·mL^{-1}); V is the volume of the solution (mL); and W is the weight of adsorbent (g).

2.4. Desorption and Regeneration. To investigate the desorption ability of adsorbed Hg(II) ions from four adsorbents, desorption experiments were carried out as follows: After adsorption, the Hg(II) ion loaded adsorbents were separated and slightly washed with distilled water to remove unadsorbed Hg(II) ions on the surface of the adsorbents. They were stirred with 20 mL of 0.1 mol·L^{-1} HNO_3 containing various thiourea concentrations ranging from (0 to 5) % for 6 h, and the concentrations of Hg(II) ions were analyzed as before. The desorption ratio of Hg(II) ions was then calculated as the ratio of the amount of desorbed Hg(II) ions to the amount of initially adsorbed Hg(II) ions. To test the reusability of the adsorbents, adsorption−desorption cycles were repeated 5 times by using the same adsorbent.

3. Results and Discussion

3.1. Adsorption Kinetics. The kinetics of adsorption that describes the solute uptake rate governing the contact time of the adsorption reaction was one of the important characteristics that define the efficiency of adsorption. Hence, in the present study, the kinetics of Hg(II) ions removal was determined to understand the adsorption behavior of SG-HE-dD, SG-HO-dD, SG-HE-pD, and SG-HO-pD, and the effect of contact time at different temperatures [(10, 20, 30, and 40) °C] is shown in Figure 1. When adsorbents prepared by different methods were used for the adsorption kinetics of Hg(II) ions, the order of adsorption capacities was: SG-HO-pD > SG-HO-dD > SG-HE-pD > SG-HE-dD, indicating the homogeneous method and end-group protection method were favorable for preparing highly effective adsorbents with higher adsorption capacities, especially the end-group protection method. In the case of SG-HO-dD and SG-HO-pD, the adsorption capacities for Hg(II) ions were

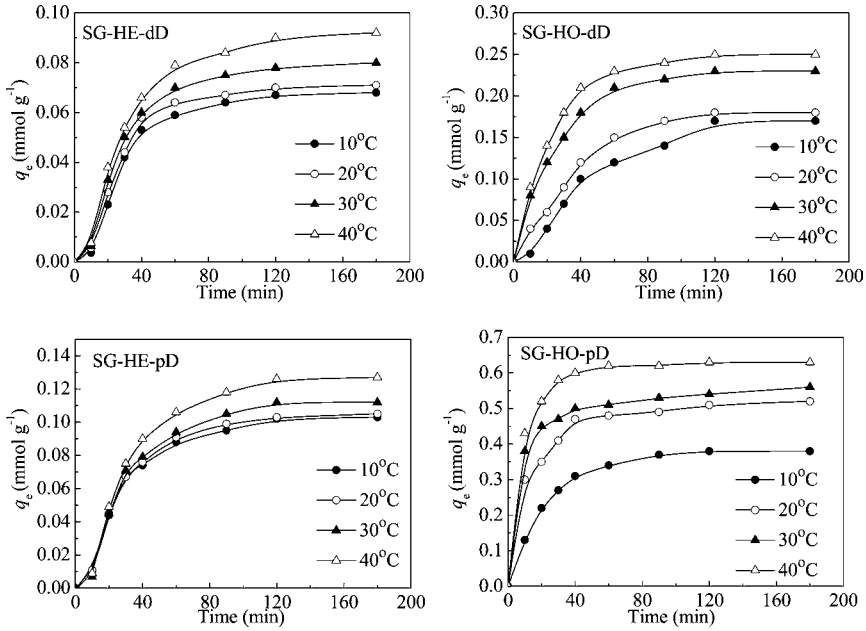

Figure 1. Adsorption kinetics of Hg(II) ions onto SG-HE-dD, SG-HO-dD, SG-HE-pD, and SG-HO-pD. Adsorption conditions: initial concentration of Hg(II) ions, $5 \cdot 10^{-3}$ mol·L^{-1}, pH 4.0.

inconsistent with the content of N. The reason for this is that the adsorbents prepared by the end-group protection method contained dispersing ligand units that gave rise to better coordination with Hg(II) ions. For SG-HE-dD and SG-HE-pD, the adsorption results were also similar to SG-HO-dD and SG-HO-pD.

As shown in Figure 1, the adsorption capacities of SG-HE-dD, SG-HO-dD, SG-HE-pD, and SG-HO-pD for Hg(II) ions increased with increasing temperature. These findings suggest that at lower temperatures the Hg(II) ions were easily solvated by water molecules to form a hydrated ion, which was bigger and more difficult to diffuse into the porous silica-gel matrix than the bare Hg(II) ions. In contrast, at higher temperatures, the hydrated Hg(II) ions were dissolved to produce the bare Hg(II) ions, which more easily diffused into the pores of the silica-gel matrix. Thus, adsorption relies not only on the surface adsorption but also on the porous structure of the silica-gel matrix. The kinetic curves of SG-HE-dD, SG-HO-dD, SG-HE-pD, and SG-HO-pD for Hg(II) showed that the adsorption was rapid for the first 40 min and then slowed considerably. It was noteworthy that SG-HO-pD required only 60 min to reach adsorption equilibrium, and SG-HE-dD and SG-HO-dD and SG-HE-pD at least 120 min, which may be interpreted as having remaining large pore diameters and dispersive ligand units.[21] Hence, in the present study, we used 240 min contact time for further experiments to ensure complete adsorption.

Following Boyd et al.[23] and Reichenberg,[24] the adsorption procedure of adsorbents for metal ions was considered to take place through two mechanisms of film diffusion and particle diffusion. Film diffusion was rate controlling when the absorbent was exposed to a low metal ion concentration, and particle diffusion might be rate controlling when exposed to a high metal ion concentration. Kinetic data were analyzed by the procedure given by Reichenberg[24] and Helfferich.[25] The following equations were used

$$F = 1 - \frac{6}{\pi^2}\sum_{n=1}^{\infty}\frac{1}{n^2}\left[\frac{-D_i t\pi^2 n^2}{r_0^2}\right] \tag{2}$$

or

$$F = 1 - \frac{6}{\pi^2}\sum_{n=1}^{\infty}\frac{1}{n^2}\exp[-n^2 Bt] \tag{3}$$

where n is an integer that defines the infinite series solution and F is the fractional attainment of equilibrium at time t and is obtained by the expression

$$F = \frac{q_t}{q_e} \tag{4}$$

where q_t is the amount of metal ions taken up at time t and q_e is the amount of metal ion adsorbed at equilibrium and

$$B = \frac{\pi^2 D_i}{r_0^2} = \text{time constant} \tag{5}$$

where D_i is the effective diffusion coefficient of the ion in the adsorbent phase, and r_0 is the radius of the adsorbent particle assumed to be spherical.

Values of Bt were obtained from corresponding values of F. Bt values for each F are given by Reichenberg,[24] and the results were plotted in Figure 2.

The linearity of this plot is employed to distinguish between external-transport- (film diffusion) and intraparticle-transport-controlled rates of adsorption.[26] A straight line passing through the origin is indicative of adsorption processes governed by particle-diffusion mechanisms; otherwise, they might be governed by film diffusion.[27]

As shown in Figure 3, in all the cases studied, all the lines of the relationship between Bt and t were linear but without passing through the origin, suggesting film diffusion, rather than particle diffusion, is the rate-limiting adsorption process of SG-HE-dD, SG-HO-dD, SG-HE-pD, and SG-HO-pD for Hg(II) ions. The linear equations and coefficients of determination R^2 are given in Table 1.

Pseudofirst-order[28] and pseudosecond-order[29] equations were used to test the experimental data and thus elucidate the adsorption kinetic process. The pseudofirst-order model is expressed as

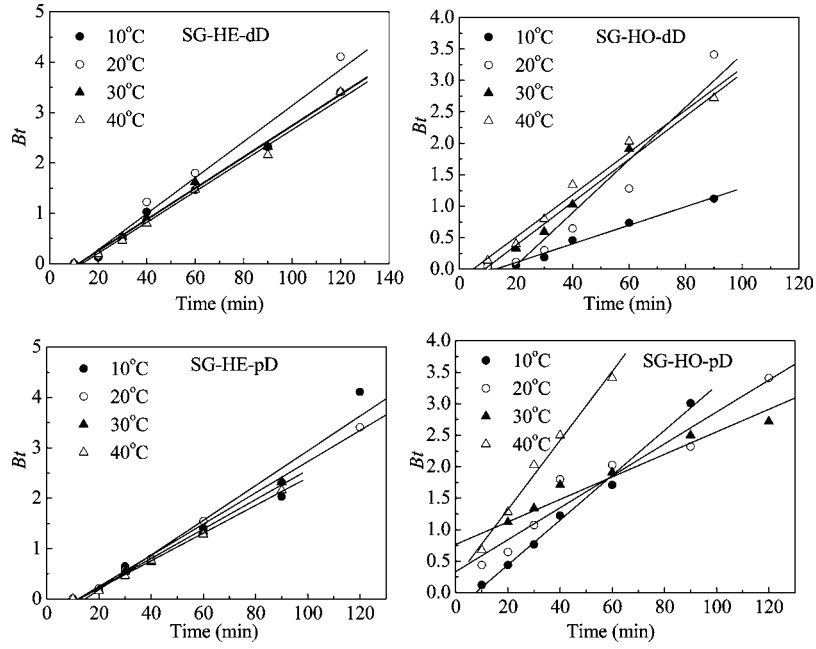

Figure 2. *Bt* vs time plots at different adsorbate temperatures of Hg(II) ions onto SG-HE-dD, SG-HO-dD, SG-HE-pD, and SG-HO-pD.

$$\ln \frac{(q_e - q_t)}{q_e} = -k_1 t \quad (6)$$

where k_1 is the pseudofirst-order rate constant (min^{-1}) of adsorption and q_e and q_t ($mmol \cdot g^{-1}$) are the amounts of metal ion adsorbed at equilibrium and time t (min), respectively. The value of $\ln(q_e - q_t)$ was calculated from the experimental results and plotted against t (min). The experimental and calculated q_e values, pseudofirst-order rate constants, and regression coefficient (R_1^2) values are presented in Table 2.

The pseudosecond-order model can be expressed as

$$\frac{t}{q_t} = \frac{1}{k_2 q_e^2} + \frac{t}{q_e} \quad (7)$$

where k_2 is the pseudosecond-order rate constant of adsorption ($g \cdot mmol^{-1} \cdot min^{-1}$). The slope and intercept of the linear plot t/q_t vs t yielded the values of q_e and k_2.

As can be seen from Table 2, the pseudofirst-order model fit the data very well and provided better correlation coefficients than the pseudosecond-order model for SG-HE-dD, SG-HO-dD, and SG-HE-pD, suggesting the pseudofirst-order model was more suitable to describe the adsorption kinetics of Hg(II) ions onto SG-HE-dD, SG-HO-dD, and SG-HE-pD. Moreover, the calculated q_e values depending on the pseudofirst-order model were in good agreement with the experimental values q_e(exp). However, the results demonstrated that there was no significant relationship between the kinetic data (figure not shown) of SG-HO-pD with a low correlation coefficient (< 0.950), indicating that the pseudofirst-order model is not applicable to describe the adsorption of Hg(II) ions onto SG-HO-pD.

The regression coefficient (R_2^2) and several parameters obtained from the pseudosecond-order kinetic model are also shown in Table 2. As seen from Table 2, the obtained R_2^2 values for the adsorption of Hg(II) ions onto SG-HO-pD are above 0.996. Moreover, the calculated q_e values are in good agreement with experimental values q_e(exp). Hence, the adsorption kinetics could well be approximated more favorably by a pseudosecond-order kinetic model for Hg(II) ions onto SG-HO-pD. This model assumes that two reactions are occurring: the first one is fast and reaches equilibrium quickly, and the second is a slower reaction that can continue for long time periods. The reactions can occur either in series or in parallel.[30]

The adsorption rate is one of the important kinetic parameters. It can be observed from Table 2. The values of k_1 for SG-HE-dD and SG-HE-pD decreased with increasing temperature, while the values of k_1 for SG-HO-dD and k_2 for SG-HO-pD increased with increasing temperature. The initial adsorption rate, h, has been widely used for evaluation of the adsorption rates. On the basis of the pseudofirst-order model, the initial adsorption rates (h_1, $mmol \cdot g^{-1} \cdot h^{-1}$) of the SG-HE-dD, SG-HO-dD, and SG-HE-pD for Hg(II) ions at

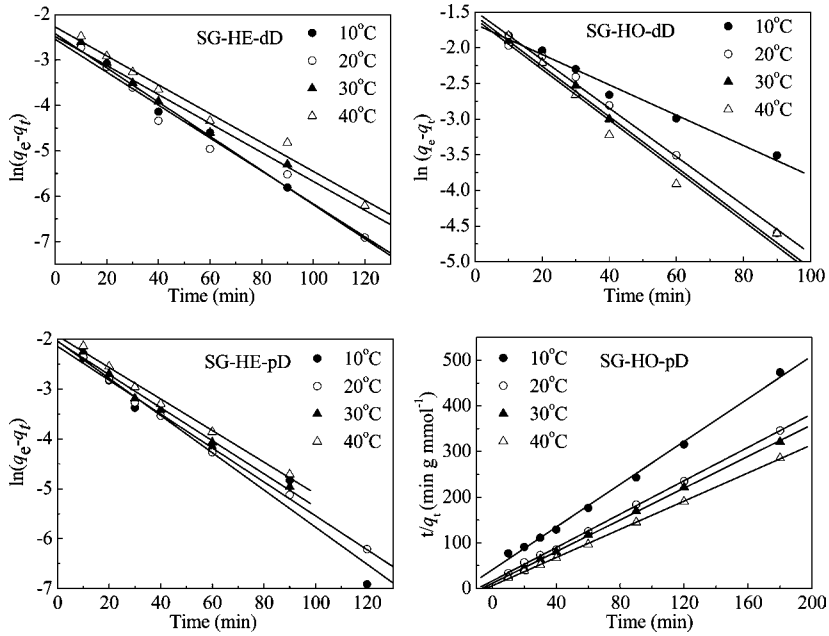

Figure 3. Pseudofirst-order kinetic plots for the adsorption of Hg(II) ions onto SG-HE-dD, SG-HO-dD, and SG-HE-pD and pseudosecond-order kinetic plots for that onto SG-HO-pD.

Table 1. *Bt* versus Time Linear Equations and Coefficients R^2

adsorbents	temperature, °C	linear equation	coefficient of determination, R^2
SG-HE-dD	10	$Bt = 0.03110t - 0.3739$	0.9935
	30	$Bt = 0.0311t - 0.3616$	0.9956
	40	$Bt = 0.0307t - 0.4077$	0.9920
SG-HO-dD	10	$Bt = 0.0148t - 0.0189$	0.9856
	30	$Bt = 0.0342t - 0.0306$	0.9886
	40	$Bt = 0.0336t - 0.1636$	0.9814
SG-HE-pD	10	$Bt = 0.0345t - 0.5071$	0.9478
	30	$Bt = 0.0292t - 0.3645$	0.9949
	40	$Bt = 0.0275t - 0.3407$	0.9970
SG-HO-pD	10	$Bt = 0.0356t - 0.2718$	0.9932
	30	$Bt = 0.0179t + 0.7647$	0.9432
	40	$Bt = 0.0549t + 0.2231$	0.9879

Table 2. Kinetic Parameters for the Adsorption of Hg(II) Ions onto SG-HE-dD, SG-HO-dD, SG-HE-pD, and SG-HO-pD Adsorbents at Various Temperatures

			pseudofirst-order kinetics				pseudosecond-order kinetics			
	T	q_e(exp)	k_1	q_e(cal)	h_1		k_2	q_e(cal)	h_2	
adsorbents	(°C)	(mmol·g^{-1})	(min^{-1})	(mmol·g^{-1})	(mmol·g^{-1}·h^{-1})	R_1^2	(g·mmol^{-1}·min^{-1})	(mmol·g^{-1})	(mmol·g^{-1}·h^{-1})	R_2^2
SG-HE-dD	10	0.068	0.037	0.088	0.0025	0.9949	0.037	0.16	-	0.1974
	20	0.071	0.036	0.078	0.0026	0.9761	0.10	0.12	-	0.5566
	30	0.080	0.032	0.083	0.0026	0.9875	0.09	0.13	-	0.5656
	40	0.092	0.032	0.10	0.0029	0.9832	0.08	0.14	-	0.6143
SG-HO-dD	10	0.17	0.021	0.18	0.0036	0.9834	0.010	0.45	-	0.2544
	20	0.18	0.034	0.22	0.0061	0.9927	0.097	0.23	-	0.9766
	30	0.23	0.035	0.21	0.0081	0.9845	0.19	0.26	-	0.9958
	40	0.25	0.035	0.20	0.0089	0.9754	0.23	0.28	-	0.9973
SG-HE-pD	10	0.103	0.037	0.13	0.0037	0.9612	0.10	0.15	-	0.7336
	20	0.105	0.034	0.12	0.0037	0.9961	0.11	0.15	-	0.7709
	30	0.112	0.033	0.13	0.0037	0.9903	0.028	0.24	-	0.3052
	40	0.127	0.032	0.14	0.0041	0.9920	0.042	0.23	-	0.4671
SG-HO-pD	10	0.38	0.039	0.36	-	0.9951	0.13	0.43	0.019	0.9965
	20	0.52	0.026	0.24	-	0.9341	0.20	0.55	0.054	0.9994
	30	0.56	0.019	0.16	-	0.9499	0.27	0.57	0.085	0.9996
	40	0.63	0.039	0.31	-	0.8623	0.40	0.65	0.16	0.9997

Table 3. Thermodynamic Parameters of SG-HE-dD, SG-HO-dD, SG-HE-pD, and SG-HO-pD for Hg(II) Ion Adsorption

	T	$\Delta G°$	$\Delta H°$	$\Delta S°$
adsorbents	(K)	(kJ·mol^{-1})	(kJ·mol^{-1})	(J·K^{-1}·mol^{-1})
SG-HE-dD	283	9.11	8.48	−2.39
	293	8.06		
	303	6.80		
	313	4.71		
SG-HO-dD	283	9.26	10.49	12.64
	293	8.32		
	303	6.96		
	313	4.10		
SG-HE-pD	283	9.32	5.06	−10.79
	293	8.38		
	303	6.55		
	313	4.03		
SG-HO-pD	283	9.14	13.60	31.60
	293	8.40		
	303	6.40		
	313	3.76		

(10, 30, and 40) °C are estimated in Table 2 according to the following equation[31]

$$h_1 = k_1 q_e \tag{8}$$

The initial adsorption rate (h_2, mmol·g^{-1}·h^{-1}) of SG-HO-pD for Hg(II) ions can also be seen in Table 3 based on the pseudosecond-order-model using eq 8[31]

$$h_2 = k_2 q_e^2 \tag{9}$$

As shown in Table 2, the initial adsorption rate increases with increasing temperature for four adsorbents. For SG-HE-dD and SG-HE-pD, initial adsorption rates were higher at high temperatures, but the rate constants were lower at high temperatures. A possible explanation for this is that the diffusion rate of Hg(II) ions is enhanced initially at high temperature, and the complex quickly forms on the surface of the adsorbent and prevents other Hg(II) ions diffusing into the inside of the pores of the adsorbents, so the rate constant at the highest temperature is not the largest. The initial adsorption rates of SG-HO-dD and SG-HO-pD increased with increasing temperature when the rate was constant, while those of SG-HE-dD and SG-HE-pD decreased with increasing temperature. That might be because the functional groups on SG-HO-dD and SG-HO-pD, especially on SG-HO-pD, had good dispersion, and Hg(II) ions were still available to diffuse into the pores. The above-mentioned fact demonstrated that the homogeneous method is more beneficial than the heterogeneous one to increase the diffusion rate of metal ions into the matrix of adsorbents. Meanwhile, a combination of end-group-protection and homogeneous methods can provide the best route to prepare the adsorbents with a high metal adsorption rate.

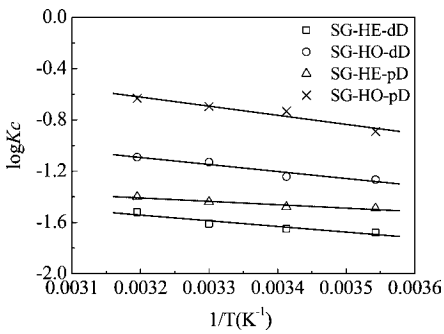

Figure 4. log K_c vs 1/T plots for Hg(II) ion adsorption onto SG-HE-dD, SG-HO-dD, SG-HE-pD, and SG-HO-pD.

A conclusion can be drawn from the kinetics study that the structures and distributions of the functional group (diethylenetriamine) on the surface of silica-gel affect significantly the adsorption kinetics behavior of adsorbents for Hg(II) ions.

3.2. Thermodynamics. The variation in temperature affects the adsorption of metal ions onto solid surfaces. In the present work, we evaluated the thermodynamic behavior of the adsorption of Hg(II) ions onto SG-HE-dD, SG-HO-dD, SG-HE-pD, and SG-HO-pD though the change in free energy ($\Delta G°$), enthalpy ($\Delta H°$), and entropy ($\Delta S°$). The thermodynamic parameters like enthalpy change ($\Delta H°$) and entropy change ($\Delta S°$) were obtained from the van't Hoff equation.

$$\log K_c = \frac{\Delta S^o}{2.303R} - \frac{\Delta H^o}{2.303RT} \tag{10}$$

where T is the absolute temperature (K); R is the gas constant (8.314 J·mol^{-1}· K^{-1}); and $\Delta S°$ (J·mol^{-1}·K^{-1}) and $\Delta H°$ (kJ·mol^{-1}) were calculated from the slope and intercept of linear plots of log K_c vs 1/T (Figure 4) for Hg(II) ions. The equilibrium constant (K_c) was calculated from the following relationship.[32] The plot shown in Figure 4 is linear over the entire range of temperatures investigated.

$$K_c = \frac{C_{Ae}}{C_e} \tag{11}$$

where C_{Ae} and C_e are the equilibrium concentrations of metal ($mg \cdot L^{-1}$) on adsorbent and in solution, respectively.

Free energy change ($\Delta G°$) was calculated from the relation

$$\Delta G° = -RT \ln K_c \tag{12}$$

where T (K) is the absolute temperature; R ($J \cdot K^{-1} \cdot mol^{-1}$) is the gas constant; and $\Delta G°$ is the standard free energy change.

The results are listed in Table 3. The positive values of $\Delta H°$ for Hg(II) ions (Table 3) suggest an endothermic nature of adsorption. This is also supported by the increase in the value of adsorption capacity of all the adsorbents with a rise in temperature. The increase in adsorption of Hg(II) ions with temperature might have been due to a change in the pore size and enhanced rate of intraparticle diffusion.[33] The negative value of entropy change ($\Delta S°$) for SG-HE-dD and SG-HE-pD resulted from the decreased randomness due to the adsorption of Hg(II) ions. The negative $\Delta S°$ values reflect that no significant change occurs in the internal structure of adsorbent material during adsorption, and the positive value of $\Delta S°$ for SG-HO-dD and SG-HO-pD showed an increase in randomness at the solid/solution interface during the adsorption of Hg(II) ions. Furthermore, positive values of $\Delta G°$ and $\Delta H°$ indicate the presence of an energy barrier in the adsorption process. Positive $\Delta G°$ values are uncommon processes. Similar adsorption processes have also been reported in ref 34. The author of this reference attributed the positive $\Delta G°$ to the activated complex in the transition state in an excited form.

3.3. Adsorption Isotherms. Adsorption data for a wide range of adsorbate concentrations are most conveniently described by adsorption isotherms. Linear regression was frequently used to determine the most fitted isotherm. However, previously, researchers have showed that, depending on the way the isotherm equation is linearized, the error distribution changes either for the worse or the better.[35] Therefore, it will be an inappropriate technique to use the linearization method for estimating the equilibrium isotherm parameters. In the present study, a comparison of the linear method and nonlinear method of three isotherms, Langmuir, Freundlich, and Redlich−Peterson, was employed to determine the adsorption isotherm parameters of Hg(II) ions onto SG-HE-dD, SG-HO-dD, SG-HE-pD, and SG-HO-pD. The adsorption isotherms for Hg(II) ions are presented in Figure 5.

The Langmuir isotherm, one of the most common isotherm models, suggests that uptake occurs on a homogeneous surface by monolayer adsorption without interaction between adsorbed molecules. This model[36] can be written as follows

$$q_e = \frac{q_{the} K_L C_e}{1 + K_L C_e} \tag{13}$$

where q_e is the adsorption capacity, $mmol \cdot g^{-1}$; C_e is the equilibrium concentration of metal ions, $mmol \cdot mL^{-1}$; q_{the} is theoretical saturation adsorption capacity, $mmol \cdot g^{-1}$; and K_L is the Langmuir constant that relates to the affinity of binding sites, $mL \cdot mmol^{-1}$. The linear expression of the Langmuir isotherm is eq 14

$$\frac{C_e}{q_e} = \frac{C_e}{q_{the}} + \frac{1}{qK_L} \tag{14}$$

Nonlinear regression and graphical methods, by plotting C_e/q_e vs C_e, were used to evaluate the Langmuir parameters.

Langmuir model parameters and fits of experimental data to the above equation are given in Table 4. From Table 4, it can be seen that the regression coefficients R^2 of linear and nonlinear Langmuir models are more than 0.96, suggesting that both linear and nonlinear Langmuir isothermal models can be used to describe the isotherm adsorption of Hg(II) ions onto SG-HE-dD, SG-HO-dD, SG-HE-pD, and SG-HO-pD under the present conditions. The regression coefficients of determination by using the linear method (R^2) are more than 0.99, indicating that the adsorption of the Hg(II) ions on SG-HE-dD, SG-HO-dD, SG-HE-pD, and SG-HO-pD fitted well with the linear Langmuir model. In other words, the adsorption of Hg(II) ions on four adsorbents has taken place at the functional groups/binding sites on the surface of the adsorbents which is regarded as monolayer adsorption. Figure 6 shows experimental data adjusted to the Langmuir model obtained by using linear methods.

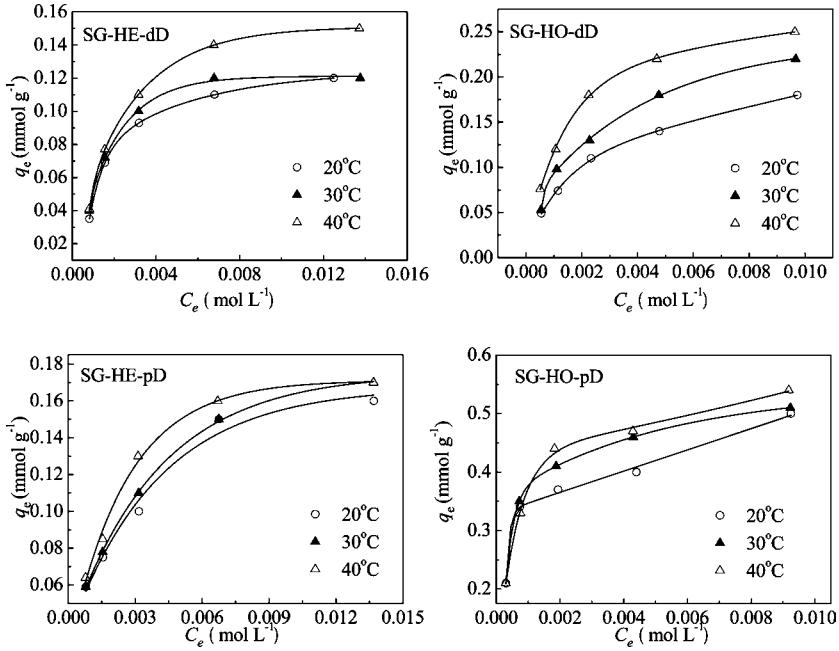

Figure 5. Isotherms for the adsorption of Hg(II) ions onto SG-HE-dD, SG-HO-dD, SG-HE-pD, and SG-HO-pD at different solution temperatures.

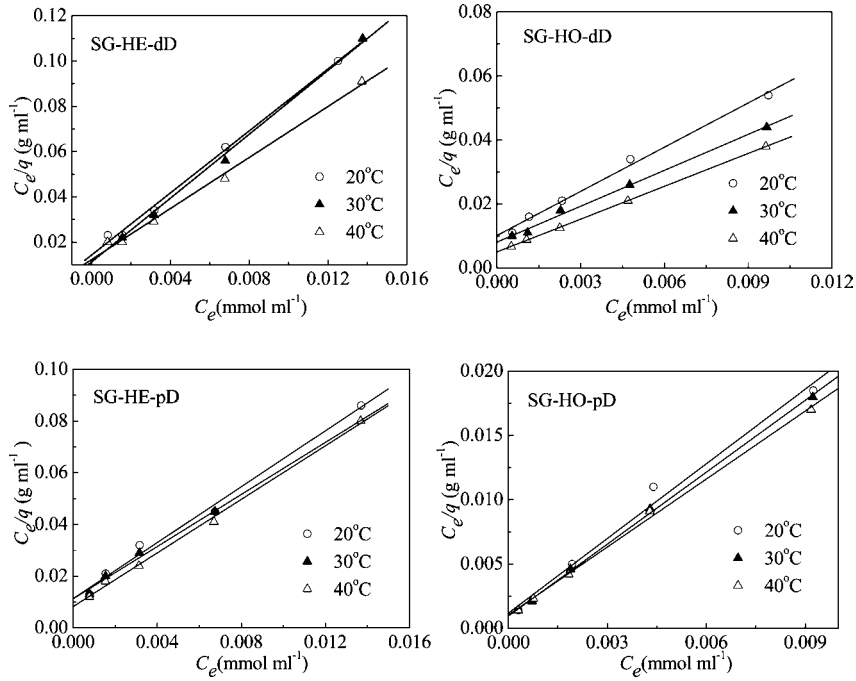

Figure 6. Langmuir isotherm obtained by using the linear method for the adsorption of Hg(II) ions onto SG-HE-dD, SG-HO-dD, SG-HE-pD, and SG-HO-pD at different temperatures by monolayer adsorption.

Table 4. Isotherm Parameters of the Langmuir Model for the Adsorption of Hg(II) Ions Obtained by Using the Linear Method and the Nonlinear Method

		langmuir					
		linear regression			nonlinear regression		
adsorbents	T (°C)	q_{the} (mmol·g^{-1})	K_L (mL·mmol^{-1})	R^2	q_{the} (mmol·g^{-1})	K_L (mL·mmol^{-1})	R^2
SG-HE-dD	20	0.14	479.31	0.9955	0.14	547.15	0.9763
	30	0.14	630.20	0.9957	0.14	637.00	0.9633
	40	0.18	458.37	0.9945	0.18	465.63	0.9854
SG-HO-dD	20	0.22	455.83	0.9937	0.21	457.89	0.9898
	30	0.27	461.95	0.9956	0.26	467.34	0.9927
	40	0.29	684.38	0.9999	0.29	703.79	0.9989
SG-HE-pD	20	0.18	478.58	0.9912	0.19	455.24	0.9634
	30	0.20	445.88	0.9967	0.19	452.41	0.9884
	40	0.19	631.84	0.9973	0.19	584.71	0.9866
SG-HO-pD	20	0.52	1613.58	0.9885	0.47	2667.33	0.9829
	30	0.54	1865.00	0.9989	0.52	2421.88	0.9795
	40	0.57	1762.60	0.9980	0.55	1995.69	0.9862

The Freundlich model was shown to be consistent with exponential distribution of active centers and the characteristics of heterogeneous surfaces by adsorption.[36] The Freundlich model is expressed as

$$q_e = K_F C_e^{1/n} \tag{15}$$

where K_F is the binding energy constant reflecting the affinity of the adsorbents to metal ions and n is the Freundlich exponent related to adsorption intensity. The linear expression of the Freundlich isotherm is eq 16

$$\ln q_e = \ln K_F + \frac{\ln C_e}{n} \tag{16}$$

The constants, K_F (mmol·g^{-1}) and n, in the Freundlich isotherm are determined by linear regression, by plotting ln q_e vs ln C_e, as well as by nonlinear regression. Table 5 shows the linear and nonlinear Freundlich adsorption isotherm constants, K_F and n, and the regression coefficients of determination, R^2. On the basis of the R^2 values, it can be seen that neither the linear form nor the nonlinear form of the Freundlich isotherm appeared to be a reasonable model for adsorption.

The Redlich−Peterson equation involves three parameters, A (L·g^{-1}), B (L·mmol^{-1}), and g ($0 < g < 1$).[37] A and B are the Redlich−Peterson isotherm constants, and g is the degree of heterogeneity. When coverage is very low, eq 15 becomes linear and leads to Henry's Law. For high coverage, eq 15 can be assimilated to the Freundlich equation,[38] since the ratio A/B and $(1 - g)$ correspond to the parameters K_F and $1/n$ of the Freundlich isotherm (eq 13). For $g = 1$, it can be assimilated to the Langmuir equation,[39] where A/B is numerically equal to the monolayer capacity (Q_0) and B is the adsorption equilibrium constant.

$$q_e = \frac{AC_e}{1 + BC_e^{\,g}} \tag{17}$$

The experimental data were fitted to the Redlich−Peterson by applying nonlinear regression analysis. The calculated isotherm constants are given in Table 6 and showed that the

Table 5. Isotherm Parameters of Freundlich for the Adsorption of Hg(II) Ions Obtained by Using the Linear Method and Nonlinear Method

		Freundlich					
		linear regression			nonlinear regression		
adsorbents	T (°C)	K_F (mmol·g^{-1})	n	R^2	K_F (mmol·g^{-1})	n	R^2
SG-HE-dD	20	0.55	3.00	0.8855	0.87	2.38	0.8632
	30	0.46	3.44	0.8265	0.72	2.67	0.8288
	40	0.72	2.87	0.8934	1.19	2.26	0.8920
SG-HO-dD	20	1.24	2.42	0.9866	0.86	2.67	0.9732
	30	1.55	2.42	0.9729	0.96	2.60	0.9817
	40	1.30	2.91	0.9408	0.89	2.79	0.9374
SG-HE-pD	20	0.75	2.87	0.9461	1.49	2.24	0.9851
	30	0.81	2.83	0.9704	2.26	2.08	0.9567
	40	0.68	3.24	0.9145	1.85	2.46	0.9410
SG-HO-pD	20	1.28	4.91	0.9071	1.42	4.52	0.8831
	30	1.39	4.87	0.9008	1.69	4.19	0.8772
	40	1.63	4.40	0.9183	2.00	3.74	0.9118

Table 6. Isotherm Parameters of the Redlich−Peterson Model for the Adsorption of Hg(II) Ions

		Redlich−Peterson			
adsorbents	T (°C)	A (L·g^{-1})	B (L·mmol$^{-1)}$)	g	R^2
SG-HE-dD	20	76.57	547.05	1.0	0.9763
	30	89.96	636.94	1.0	0.9633
	40	83.28	465.64	1.0	0.9854
SG-HO-dD	20	479.36	500.52	0.65	0.9922
	30	154.18	340.34	0.88	0.9955
	40	202.39	703.80	1.0	0.9989
SG-HE-pD	20	111.00	377.33	0.89	0.9666
	30	116.45	368.11	0.88	0.9923
	40	114.25	584.71	1.0	0.9866
SG-HO-pD	20	2428.78	2901.14	0.88	0.9892
	30	1423.83	2328.49	0.97	0.9819
	40	1279.20	1882.76	0.96	0.9891

Table 7. Regeneration Properties of SG-HE-dD, SG-HO-dD, SG-HE-pD, and SG-HO-pD

	adsorption capacity (mmol·g^{-1})			
regeneration times	SG-HE-dD	SG-HO-dD	SG-HE-pD	SG-HO-pD
1	0.75	0.91	0.81	1.73
2	0.73	0.94	0.79	1.70
3	0.72	0.91	0.71	1.64
4	0.69	0.88	0.67	1.65
5.	0.67	0.89	0.65	1.64

Redlich−Peterson model gave higher regression coefficients of determination. From Tables 4 and 6, it can be observed that the R^2 value for the Redlich−Peterson isotherm was found to be near the best-fit Langmuir isotherm equation. In addition, Tables 4 and 6 show that the regression correlation coefficients of the Redlich−Peterson and Langmuir isotherms have the same values in some cases and seem to be the best-fitting models for the experimental results. Thus, the Langmuir isotherm is a special case of the Redlich−Peterson isotherm when constant g is unity. Further, comparing the R^2 value of three isotherm models, it is easy to find that both the Langmuir and Redlich−Peterson are the best-fit isotherms to represent the experimental data of Hg(II) ion adsorption onto SG-HE-dD, SG-HO-dD, SG-HE-pD, and SG-HO-pD. The fact shows that the four adsorbents prepared by different methods have similar mechanisms, and all of them are attributed to monolayer adsorption and chemisorption.[40]

3.4. Desorption and Regeneration. Repeated availability is an important factor for an advanced adsorbent. The desorption of Hg(II) ions from immobilized SG-HE-dD, SG-HO-dD, SG-HE-pD, and SG-HO-pD using different concentrations of thiourea in HNO_3 solution as a stripping agent was investigated. The effect of the thiourea concentration on the desorption of Hg(II) ions from immobilized adsorbents is shown in Figure 7. It was apparent that Hg(II) ion desorption increased with increasing thiourea concentration. While the thiourea concentration of eluent was up to 5 %, the desorption ratio of Hg(II) ions for SG-HE-dD, SG-HO-dD, SG-HE-pD, and SG-HO-pD had observed maximum desorption rates of 94.5 %, 93.5 %, 100 %, and 97.5 %, respectively, and Hg(II) ions could be almost completely eluted. It is found that the percentage of Hg(II) ion desorption from SG-HE-pD and SG-HO-pD is higher than that of SG-HE-dD and SG-HO-dD. We conclude that the removal of the adsorbents prepared by the end-group protection method is easier than that of the other two adsorbents. To obtain the regeneration of the four adsorbents, sequential adsorption−desorption cycles were repeated five times by means of the same adsorbents. We choose 5 % thiourea/0.1 mol·L^{-1} HNO_3 as the eluent in the experiments of regeneration of the adsorbents. The adsorption capacities of five adsorption−desorption cycles are listed in Table 7. The adsorption capacity of the recycled SG-HE-dD, SG-HO-dD, SG-HE-pD, and SG-HO-pD can still be maintained at the (89, 98, 80, and 95) % level at the fifth cycle, respectively. Consequently, it could be concluded that SG-HO-dD and SG-HO-pD could be used more economically in an actual process.

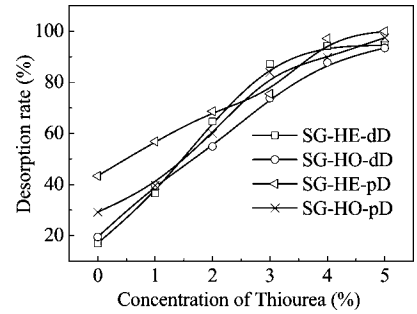

Figure 7. Effects of different concentrations of thiourea on the desorption rate (%).

4. Conclusions

The present study focuses on the adsorption of Hg(II) ions onto SG-HE-dD, SG-HO-dD, SG-HE-pD, and SG-HO-pD, and the following conclusions were drawn:

(1) The adsorption kinetic processes studied indicated that the pseudofirst-order rate model provided an excellent fitting for Hg(II) ion adsorption onto SG-HE-dD, SG-HO-dD, and SG-HE-pD and the pseudosecond-order model for Hg(II) ion adsorption onto SG-HO-pD. Film diffusion might be the dominant in the adsorption process of Hg(II) ions onto the four adsorbents.

(2) The thermodynamic parameter ($\Delta H°$, $\Delta S°$, and $\Delta G°$) values of Hg(II) ion adsorption onto SG-HE-dD, SG-HO-dD, SG-HE-pD, and SG-HO-pD show endothermic heat of adsorption, favored at high temperatures. The negative $\Delta S°$ values for SG-HE-dD and SG-HE-pD prepared by the heterogeneous method reflect that no significant change occurs in the internal structure of adsorbent material during adsorption. The positive value of $\Delta S°$ for SG-HO-dD and SG-HO-pD showed an increase in randomness at the solid/solution interface during the adsorption of Hg(II) ions.

(3) The regression coefficients of determination are found to be more than 0.96, and the linear Langmuir and nonlinear Langmuir and Redlich−Peterson isotherm models provide the

best fits to predict the adsorption equilibrium for Hg(II) ions onto SG-HE-dD, SG-HO-dD, SG-HE-pD, and SG-HO-pD. The Redlich−Peterson model is a special case of the Langmuir model when the Redlich−Peterson isotherm constant g is unity.

(4) The maximum desorption rates of Hg(II) ions on SG-HE-dD, SG-HO-dD, SG-HE-pD, and SG-HO-pD of 94.5 %, 93.5 %, 100 %, and 97.5 %, respectively, have been observed. The adsorbents can be regenerated efficiently, which will enable them to be used for at least five cycles.

Literature Cited

(1) Guibal, E. Interactions of metal ions with chitosan-based sorbents: a review. *Sep. Purif. Technol.* **2004**, *38*, 43–74.
(2) Ruparelia, J. P.; Duttagupta, S. P.; Chatterjee, A. K.; Mukherji, S. Potential of carbon nanomaterials for removal of heavy metals from water. *Desalination* **2008**, *232*, 145–156.
(3) Deligöz, H.; Erdem, E. Comparative studies on the solvent extraction of transition metal cations by calixarene, phenol and ester derivatives. *J. Hazard. Mater.* **2008**, *154*, 29–32.
(4) Vijayalakshmi, A.; Arockiasamy, D. L.; Nagendran, A.; Mohan, D. Separation of proteins and toxic heavy metal ions from aqueous solution by CA/PC blend ultrafiltration membranes. *Sep. Purif. Technol.* **2008**, *62*, 32–38.
(5) Atia, A. A.; Donia, A. M.; Elwakeel, K. Z. Selective separation of mercury (II) using a synthetic resin containing amine and mercaptan as chelating groups. *React. Funct. Polym.* **2005**, *65*, 267–275.
(6) Türker, A. R. New sorbents for solid-phase extraction for metal enrichment. *Clean* **2007**, *35*, 548–557.
(7) Jal, P. K.; Patel, S.; Mishra, B. K. Chemical modification of silica surface by immobilization of functional groups for extractive concentration of metal ions. *Talanta* **2004**, *62*, 1005–1028.
(8) Hassanien, M. M.; Abou-El-Sherbini, K. S. Synthesis and characterisation of morin-functionalised silica gel for the enrichment of some precious metal ions. *Talanta* **2006**, *68*, 1550–1559.
(9) Lam, K. F.; Yeung, K. L.; Mckay, G. Efficient approach for Cd^{2+} and Ni^{2+} removal and recovery using mesoporous adsorbent with tunable selectivity. *Environ. Sci. Technol.* **2007**, *41*, 3329–3334.
(10) Gübbük, H.; Güp, R.; Ersöz, M. Synthesis, characterization, and sorption properties of silica gel-immobilized Schiff base derivative. *J. Colloid Interface Sci.* **2008**, *320*, 376–382.
(11) Gao, B. J.; An, F. Q.; Liu, K. K. Studies on chelating adsorption properties of novel composite material polyethyleneimine/silica gel for heavy-metal ions. *Appl. Surf. Sci.* **2006**, *253*, 1946–1952.
(12) Sales, J. A. A.; Prado, A. G. S.; Airoldi, C. The incorporation of propane-1,3-diamine into silylant epoxide group through homogeneous and heterogeneous routes. *Polyhedron* **2002**, *21*, 2647–2651.
(13) Sales, J. A. A.; Airoldi, C. Calorimetric investigation of metal ion adsorption on 3-glycidoxypropyltrimethylsiloxane + propane-1,3-diamine immobilized on silica gel. *Thermochim. Acta* **2005**, *427*, 77–83.
(14) Yoshitake, H.; Koiso, E.; Horie, H.; Yoshimura, H. Polyamine-functionalized mesoporous silicas: Preparation, structural analysis and oxyanion adsorption. *Microporous Mesoporous Mater.* **2005**, *85*, 183–194.
(15) Liu, C. K.; Bai, R. B.; Hong, L. Diethylenetriamine-grafted poly(glycidyl methacrylate) adsorbent for effective copper ion adsorption. *J. Colloid Interface Sci.* **2006**, *303*, 99–108.
(16) Liu, C. K.; Bai, R. B.; Ly, Q. S. Selective removal of copper and lead ions by diethylenetriamine-functionalized adsorbent: Behaviors and mechanisms. *Water Res.* **2008**, *42*, 1511–1522.
(17) Atia, A. A.; Donia, A. M.; Awed, H. A. Synthesis of magnetic chelating resins functionalized with tetraethylenepentamine for adsorption of molybdate anions from aqueous solutions. *J. Hazard. Mater.* **2008**, *155*, 100–108.
(18) Suzuki, T. M.; Yokoyama, T. Preparation and complexation properties of polystyrene resins containing diethylenetriamine derivatives. *Polyhedron* **1984**, *3*, 939–945.
(19) Sales, J. A. A.; Prado, A. G. S.; Airoldi, C. Thermodynamic data for divalent cations onto new modified glycidoxy silica surface at solid/liquid interface. *J. Therm. Anal. Calorim.* **2002**, *70*, 135–141.
(20) Sales, J. A. A.; Airoldi, C. Epoxide silylant agent ethylenediamine reaction product anchored on silica gel-thermodynamics of cation-nitrogen interaction at solid/liquid interface. *J. Non-Cryst. Solids* **2003**, *330*, 142–149.
(21) Zhang, Y.; Qu, R. J.; Sun, C. M.; Qu, B. H.; Sun, X. Y.; Ji, C. N. End-group protection as a novel strategy to prepare silica-gel supported diethylenetriamine with high adsorption capacities for metal ions. *J. Non-Cryst. Solids* **2009**, *355*, 453–457.
(22) Zhang, Y.; Qu, R. J.; Sun, C. M.; Wang, C. H.; Ji, C. N.; Chen, H.; Yin, P. Chemical modification of silica-gel with diethylenetriamine via an end-group protection approach for adsorption to Hg(II). *Appl. Surf. Sci.* **2009**, *255*, 5818–5826.
(23) Boyd, G. E.; Adamson, A. W.; Myers, L. S. The exchange adsorption of ions from aqueous solutions by organic zeolites. II. Kinetics. *J. Am. Chem. Soc.* **1947**, *69*, 2836–2848.
(24) Reichenberg, D. Properties of ion-exchange resins in relation to their structure III, kinetics of exchange. *J. Am. Chem. Soc.* **1953**, *75*, 589–592.
(25) Helfferich, F. *Ion-Exchange*; McGraw-Hill: New York, 1962.
(26) Mohan, D.; Singh, K. P. Single- and multi-component adsorption of cadmium and zinc using activated carbon derived from bagasse-an agricultural waste. *Water Res.* **2006**, *36*, 2304–2318.
(27) El-Kamash, A. M.; Zaki, A. A.; Abed-El-Geleel, M. Modeling batch kinetics and thermodynamics of zinc and cadmium removal from waste solutions using synthetic zeolite. *J. Hazard. Mater.* **2005**, *127*, 211–220.
(28) Barkat, M.; Nibou, D.; Chegrouche, S.; Mellah, A. Kinetics and thermodynamics studies of chromium(VI) ions adsorption onto activated carbon from aqueous solutions. *Chem. Eng. Process.* **2009**, *48*, 38–47.
(29) Ho, Y. S.; McKay, G.; Wase, D. A. J.; Foster, C. F. Study of the sorption of divalent metal ions on to peat. *Adsorp. Sci. Technol.* **2000**, *18*, 639–650.
(30) Brusseau, M. L.; Rao, P. S. C. Sorption non-ideality during organic contaminant transport in porous media. *CRC Crit. Rev. Environ. Control.* **1984**, *19*, 33–99.
(31) Amarasinghe, B. M. W. P. K.; Williams, R. A. Tea waste as a low cost adsorbent for the removal of Cu and Pb from wastewater. *Chem. Eng. J.* **2007**, *132*, 299–309.
(32) Rao, R. A. K.; Khan, M. A. Biosorption of bivalent metal ions from aqueous solution by an agricultural waste: Kinetics, thermodynamics and environmental effects. *Colloids Surf. A* **2009**, *332*, 121–128.
(33) Benhammon, A.; Yaacoubi, A.; Nibou, L.; Tanonti, B. Adsorption of metal ions onto Moroccan stevensite: kinetic and isotherm studies. *J. Colloids Interface Sci.* **2005**, *282*, 320–326.
(34) Chang, Y. C.; Chen, D. H. Recovery of gold(III) ions by a chitosan-coated magnetic nano-adsorbent. *Gold Bull.* **2006**, *39*, 98–102.
(35) Kumar, K. V.; Sivanesn, S. Comparative analysis of linear and non-linear method of estimating the sorption isotherm parameters for malachite green onto activated carbon. *J. Hazard. Mater. B* **2006**, *136*, 197–202.
(36) Ramesh, A.; Hasegawa, H.; Sugimoto, W.; Maki, T.; Ueda, K. Adsorption of gold(III), platinum(IV) and palladium(II) onto glycine modified crosslinked chitosan resin. *Bioresour. Technol.* **2008**, *99*, 3801–3809.
(37) Redlich, O.; Peterson, D. L. A useful adsorption isotherm. *J. Phys. Chem.* **1959**, *63*, 1024–1024.
(38) Zhou, M. L.; Martin, G.; Taha, S.; Sant'anna, F. Adsorption isotherm comparison and modelling in liquid phase onto activated carbon. *Water Res.* **1996**, *32*, 1109–1118.
(39) Ho, Y. S.; Huang, C. T.; Huang, H. W. Equilibrium sorption isotherm for metal ions on tree fern. *Process Biochem.* **2002**, *37*, 1421–1430.
(40) Sun, C. M.; Qu, R. J.; Ji, C. N.; Wang, C. H.; Sun, Y. Z.; Yue, Z. W.; Cheng, G. X. Preparation and adsorption properties of crosslinked polystyrene-supported low-generation diethanolamine-typed dendrimer for metal ions. *Talanta* **2006**, *70*, 14–19.

Received for review August 3, 2009. Accepted November 28, 2009. The authors are grateful for the financial support by the Nature Science Foundation of Shandong Province (No. ZR2009FM075, 2008BS04011, Y2007B19), the Nature Science Foundation of Ludong University (No.08-CXA001, 032912, 042920, LY20072902), Educational Project for Postgraduate of Ludong University (No. Ycx0612).

JE900654E